ACCOUNTS
of chemical research

Chlorophyll J-Aggregates: From Bioinspired Dye Stacks to Nanotubes, Liquid Crystals, and Biosupramolecular Electronics

SANCHITA SENGUPTA[§] AND FRANK WÜRTHNER*

Institut für Organische Chemie and Center for Nanosystems Chemistry, Universität Würzburg, Am Hubland, 97074 Würzburg, Germany

RECEIVED ON JANUARY 25, 2013

CONSPECTUS

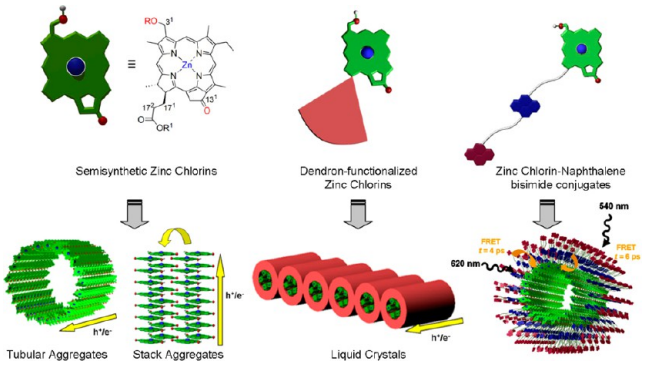

Among the natural light-harvesting (LH) systems, those of green sulfur and nonsulfur photosynthetic bacteria are exceptional because they lack the support of a protein matrix. Instead, these so-called chlorosomes are based solely on "pigments". These are self-assembled bacteriochlorophyll *c*, *d*, and *e* derivatives, which consist of a chlorophyll skeleton bearing a 3^1-hydroxy functional group. Chemists consider the latter as an essential structural unit to direct the formation of light-harvesting self-assembled dye aggregates with J-type excitonic coupling. The intriguing properties of chlorosomal J-type aggregates, particularly narrow red-shifted absorption bands, compared with monomers and their ability to delocalize and migrate excitons, have inspired intense research activities toward synthetic analogues in this field. The ultimate goal of this research field is the development of (opto-)electronic devices based on the architectural principle of chlorosomal LH systems. In this regard, the challenge is to develop small, functional building blocks with appropriate substituents that are preprogrammed to self-assemble across different length scales and to emulate functions of natural LH systems or to realize entirely new functions beyond those found in nature. In this Account, we highlight our achievements in the past decade with semisynthetic zinc chlorins (ZnChls) as model compounds of bacteriochlorophylls obtained from the naturally most abundant chlorin precursor: chlorophyll *a*.

To begin, we explore how supramolecular strategies involving π-stacking, hydrogen bonding, and metal−oxygen coordination can be used to design ZnChl-based molecular stack, tube, and liquid crystalline assemblies conducive to charge and energy transport. Our design principle is based on the bioinspired functionalization of the 3^1-position of ZnChl with a hydroxy or methoxy group; the former gives rise to tubular assemblies, whereas the latter induces stack assemblies. Functionalization of the 17^2-position with esterified hydrophilic or hydrophobic chains, dendron-wedge substituents, and chromophores having complementary optical properties such as naphthalene bisimides (NBIs) is used to modulate the self-assembly of ZnChl dyes. The resulting assemblies exhibit enhanced charge transport and energy transfer abilities. We have used UV/vis, circular dichroism (CD), fluorescence spectroscopy, and dynamic light scattering (DLS) for the characterization of these assemblies in solution. In addition, we have studied assembly morphologies by atomic force microscopy (AFM), scanning tunneling microscopy (STM), transmission electron microscopy (TEM), and cryogenic-TEM. Crystallographic techniques such as powder X-ray and solid-state NMR have been used to explain the precise long- and short-range packing of dyes in these assemblies. Finally, functional properties such as charge and energy transport have been explored by pulse radiolysis time-resolved microwave conductivity (PR-TRMC), conductive AFM, and time-resolved fluorescence spectroscopy. The design principles discussed in this Account are important steps toward the utilization of these materials in biosupramolecular electronics and photonics in the future.

Published on the Web 07/18/2013 www.pubs.acs.org/accounts
10.1021/ar400017u

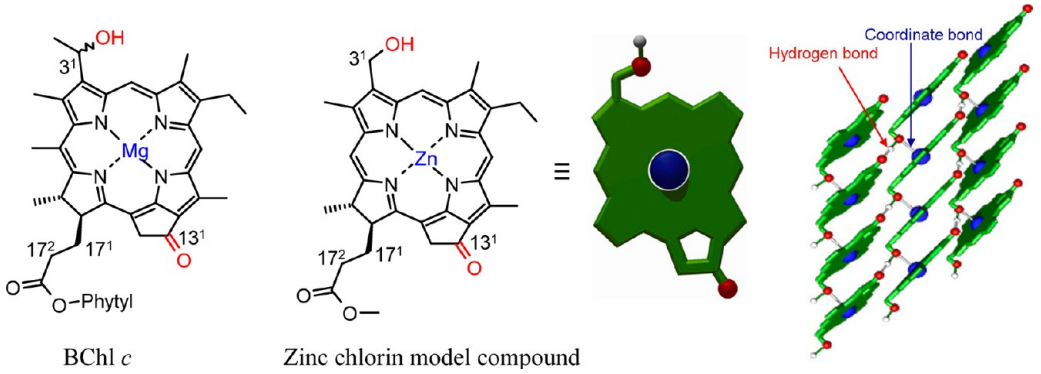

FIGURE 1. Chemical structures of BChl *c* and zinc chlorin model compound and schematic representation of a section of tubular assemblies formed by the interplay of hydrogen bonding (red arrow), metal–oxygen coordination (blue arrow), and $\pi-\pi$ stacking.

1. Introduction

Nature has created fascinating complex supramolecular architectures that are vital for sustaining life. One of the most prominent examples is the cyclic bacteriochlorophyll (BChl) arrays[1,2] in light-harvesting (LH) complexes of purple bacteria. Inspired by this example, complex superstructures were achieved using construction principles or building blocks from nature with the expectation that architectural complexity would commensurate with functional sophistication of biological systems. For example, considerable efforts have been invested in mimicking photosynthetic BChl arrays by designing biomimetic arrays of chromophores,[3,4] particularly metalloporphyrin cyclic arrays,[5,6] to get more insight into the photophysics of energy collection and transfer to the reaction center of the photosynthetic apparatus. A synthetically less demanding protocol is to employ dye–dye interactions, as prevalent in the highly specialized LH apparatus of green sulfur bacteria, namely, chlorosomes.[7,8] Chlorosomal LH systems of green sulfur bacteria (Chlorobi), filamentous nonsulfur bacteria (Chloroflexi), and aerobic phototroph *Candidatus Chloracidobacterium thermophilum* (Acidobacteria)[9] contain ~250 000 BChls *c*–*e*.[10] The chlorosomal superstructure is established solely by self-assembly driven by noncovalent interactions without requiring proteins for structural control and proper spatial arrangement of BChl dyes. The bacteriochlorophyll (BChl) *c*, *d*, and *e* dye organization in chlorosomal LH antennae of green bacteria is proposed to be driven by metal–ligand coordination, hydrogen bonding, and $\pi-\pi$ stacking.[7] These combined interactions result in extended lamellar or tubular BChl dye assemblies that exhibit J-type[11] excitonic coupling. These dye assemblies are further packed to give an organelle with about 12 nm height, 30 nm width, and 100 nm length, surrounded by a lipid monolayer. BChl assemblies show high exciton mobilities[12] and appreciable charge transport properties,[13] indicating their potential for biosupramolecular electronic and photonic applications.

Toward the impending role of chlorosomal LH dye assemblies as active materials in (opto-)electronic devices, their extensive structural and functional characterization is an obvious prerequisite. Recent technical advances in structural biology have provided profound insights into the structure and operational mechanism of the molecular machinery of a variety of photosynthetic apparatus.[14–16] However, the exact structure of chlorosomal assemblies is still a matter of debate. Owing to inherent heterogeneity of its constituent BChls (which contain varying amounts of BChl *c*, *d*, and *e* and even different side chain modifications and stereochemistry) and the large size of chlorosomes, no atomic-level details are currently available. Over four decades, several spectroscopic, (solid-state) NMR, electron microscopic (EM), and theoretical studies have resulted in variable structural models addressing both microscopic and macroscopic organization of BChls in chlorosomal antennae; noteworthy proposed models are the tubular organization by Holzwarth and Schaffner,[17] lamellar organization by Pšenčík,[18] and multilayer cylinders by Oostergetel.[19,20] Most recently, based on mutants with strongly reduced variability, including those consisting of nearly pure 17^2-farnesyl-(*R*)-[8-ethyl,12-methyl]BChl *c*, the formation of different macroscopic morphologies has been explained by an assembly of homogeneous domains of ~40 monomers from combined solid state NMR and EM studies.[21]

The construction principle for chlorosomal self-assembly can be mimicked by using a semisynthetic 3^1-hydroxy zinc chlorin (ZnChl) model compound (see Figure 1), a BChl *d* analogue developed by Tamiaki et al. that possesses the essential structural features for tubular assembly.[22] The major advantage of ZnChls over native BChls lies in their facile semisynthetic accessibility from Chl *a* and their

SCHEME 1. Synthetic Routes and Chemical Structures of ZnChl Derivatives **1**–**10**

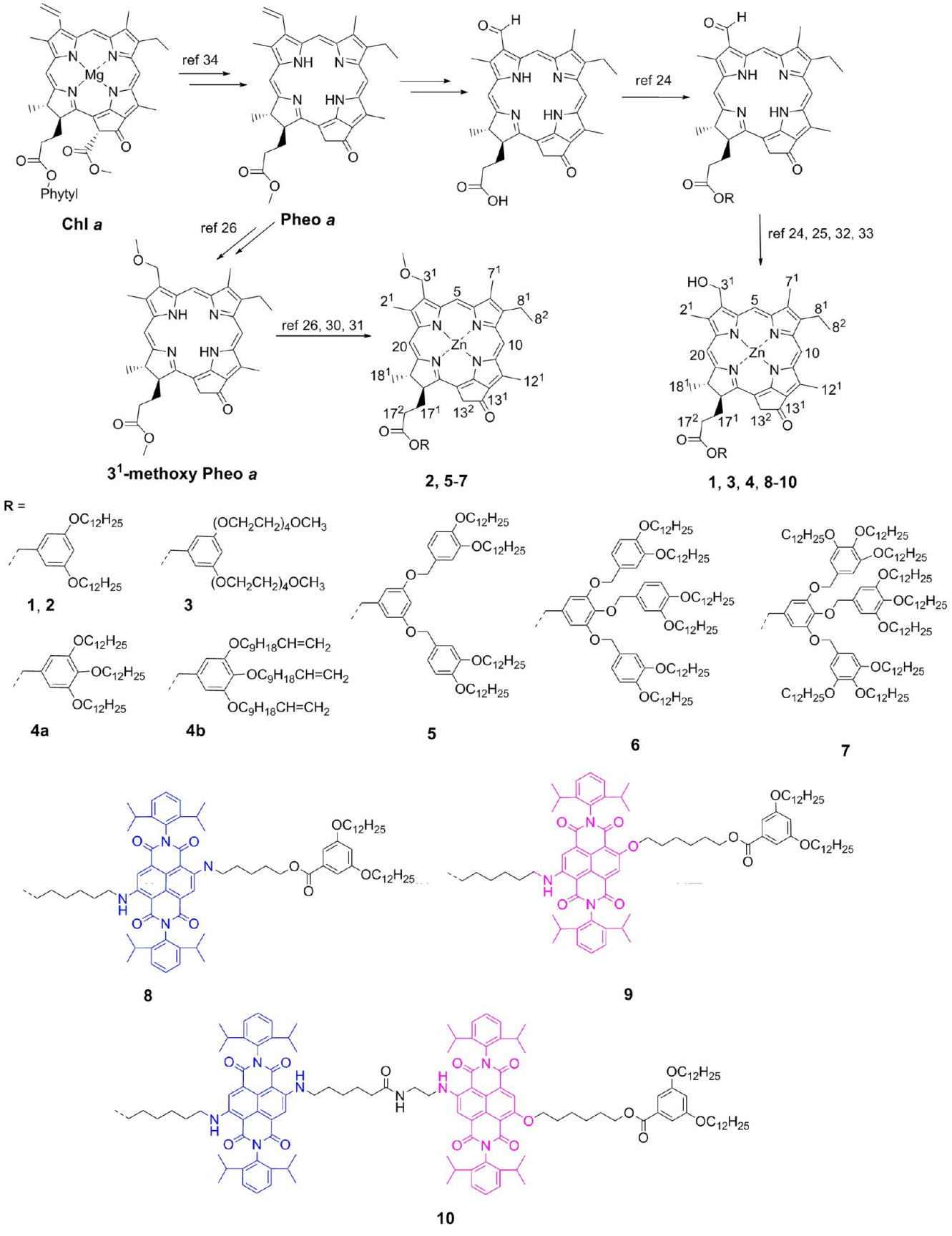

enhanced chemical stability compared with their natural Mg^{2+}-containing counterparts. Intensive investigations of aggregates of ZnChl model compounds in nonpolar solvents such as *n*-hexane or *n*-heptane revealed nearly identical spectral properties to those of the natural chlorosomal assemblies, that is, very narrow red-shifted absorption bands (~740 nm) compared with monomers (~647 nm), confirming their suitability for the imitation of chlorosomal antennae.[7] However, due to poor solubility, these in vitro aggregates were prone to precipitation, and structure–property relationships were difficult to derive.

In 2005, our group reported ZnChls functionalized with two or three dodecyl chains at the 17^2-position that afforded for the first time well-soluble rod aggregates[23] and facilitated intense spectroscopic and microscopic investigations.[24] Here we summarize our efforts in designing various ZnChl building blocks decorated with peripheral substituents for programmed self-assembly and characterization of their nanotubular, stacked, and liquid crystalline (LC) assemblies in solution, in solid state, and on surfaces. Finally, charge and energy transport properties of these biomimetic assemblies have been explored.

2. Molecular Design and Synthesis of Zinc Chlorins

To achieve the desired supramolecular arrangement and functional properties of zinc chlorins, we have functionalized them at the 3^1-carbon and 17^2-ester positions. Three different design strategies were employed to prepare semisynthetic ZnChl building blocks shown in Scheme 1. As a first approach, ZnChls were derivatized at the 3^1-position with a hydroxy[23–25] or a methoxy group[26] and sequentially decorated with two or three dodecyl,[24] undecenyl,[25] or oligo(ethylene glycol) (OEG) chains[24] through an esterified benzyl group to induce solubility in nonpolar and aqueous media, respectively. Conceptually, we envisioned that an increased number of peripheral alkyl chains should favor the tubular supramolecular arrangement (similar to cylindrical vesicles) and reduce the undesired bundling of individual aggregates of BChl *c* in vitro (Figure 2). According to our studies, this was indeed the case, and significantly improved solubility was observed for ZnChl assemblies whose building blocks were equipped with two or three solubilizing side chains at the 17^2-position[23] in comparison to assemblies of the natural counterparts (which contain, for example, one farnesyl or phytyl group) or those from ZnChl model compounds that are equipped with single alkyl or OEG chain.[27,28]

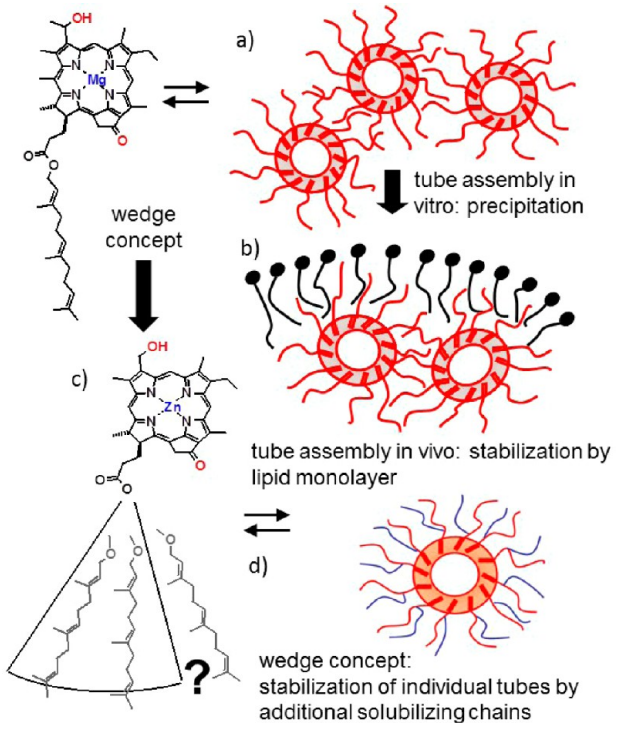

FIGURE 2. Concept of dendron wedge[29] stabilization: While natural bacteriochlorophyll *c* self-assembly in vitro leads to rapid precipitation (a) in the absence of the monolayer membrane of chlorosomes (b), an increasing number of peripheral side chains attached to the model zinc chlorin (c) stabilizes the tubular structure (d) and inhibits the bundling of the tubes and subsequent precipitation.

The hydroxy groups at the 3^1-position induce self-assembly of these dyes (ZnChls **1**, **3**, **4a**,**b**) into nanotubes similar to those proposed for natural LH chlorosomal antennae (see section 3), whereas those functionalized with 3^1-methoxy groups (ZnChl **2**) self-assemble into one- and two-dimensional stacks (see section 4). The second approach involves the variation of the ester group at the 17^2-position by enlarged dendron wedges.[29] When appended to chromophores, the defined three-dimensional shapes of the dendron wedges directly influence the organization and often induce liquid crystallinity. ZnChls **5**–**7**, which are functionalized with second-generation "Percec-type" dendron substituents, were synthesized, and their surface and bulk phase properties were investigated as discussed in sections 5 and 6.[30,31] A third design strategy was adopted to overcome the problem of so-called "green gap". Thus, multichromophoric ZnChl systems **8**–**10** were synthesized, consisting of a ZnChl unit and additional light-absorbing chromophores, particularly 2,6-core-disubstituted naphthalene bisimides (NBIs), at the 17^2-position.[32,33] The self-assembly of these multichromophoric systems and energy transfer processes of their aggregates were thoroughly investigated as discussed in section 7.[32,33]

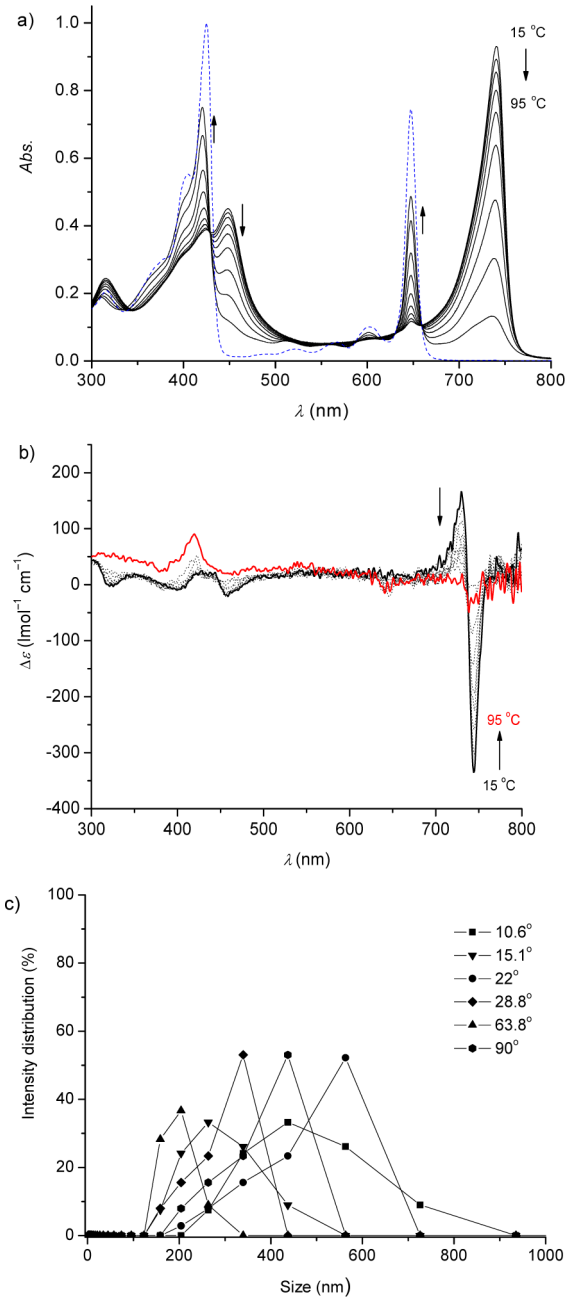

FIGURE 3. (a) Monomer spectrum of ZnChl **1** in THF (blue dotted line) and temperature-dependent UV/vis spectra (black solid lines) and (b) CD spectra of **1** in *n*-heptane/di-*n*-butyl ether (4:1) in the temperature range from 15 to 95 °C increased in 10 °C intervals. Adapted from ref 24 with permission. (c) DLS intensity distribution histogram of **1** aggregates at different scattering angles.

The deliberately designed ZnChls **1**–**10** (Scheme 1) were synthesized starting from Chl *a*, which was extracted from cyanobacteria *Spirulina platensis* according to literature procedures.[22,34] Chl *a* was converted into pheophorbide *a* according to a literature procedure,[22] and the 3^1-vinyl group was transformed into the corresponding aldehyde. The 17^2-ester functionality was hydrolyzed, followed by

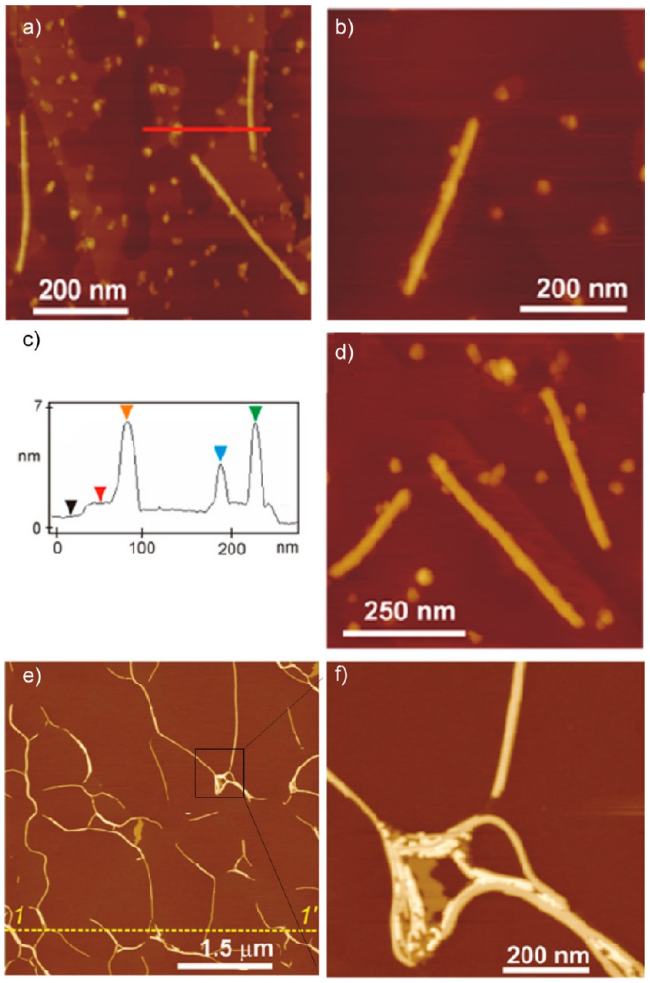

FIGURE 4. (a, b, d) Tapping-mode AFM images of nanorods of **1** spin-coated from *n*-hexane/THF (100:1) onto HOPG; (c) height profile along the red line in panel a. Panels a–d adapted from refs 23 and 24 with permission. (e) AFM image of aggregates of **3** on mica spin-coated from water/methanol (100:1; v/v) solution; (f) a magnified section of the image in panel e.

esterification with respective alcohols leading to the corresponding esters. Selective reduction of the formyl groups, followed by metalation, afforded the 3^1-hydroxy zinc chlorins **1**, **3**, **4**, and **8**–**10**. A slightly different synthetic route was adopted for the 3^1-methoxy zinc chlorins (**2**, **5**–**7**) where the pheo *a* was transformed into 3^1-methoxypheo *a*.[26] The acidic hydrolysis of the latter with concentrated hydrochloric acid and subsequent esterification of the carboxylic acid group with the respective alcohols afforded the free base esterified products. The final metalation of the free base compounds afforded the 3^1-methoxy ZnChls (**2**, **5**–**7**).

3. Tubular Assemblies: Solution and Surface Characterization

3^1-Hydroxy ZnChls **1** and **4a**,**b** functionalized with hydrophobic dodecyl or undecenyl chains self-assemble into

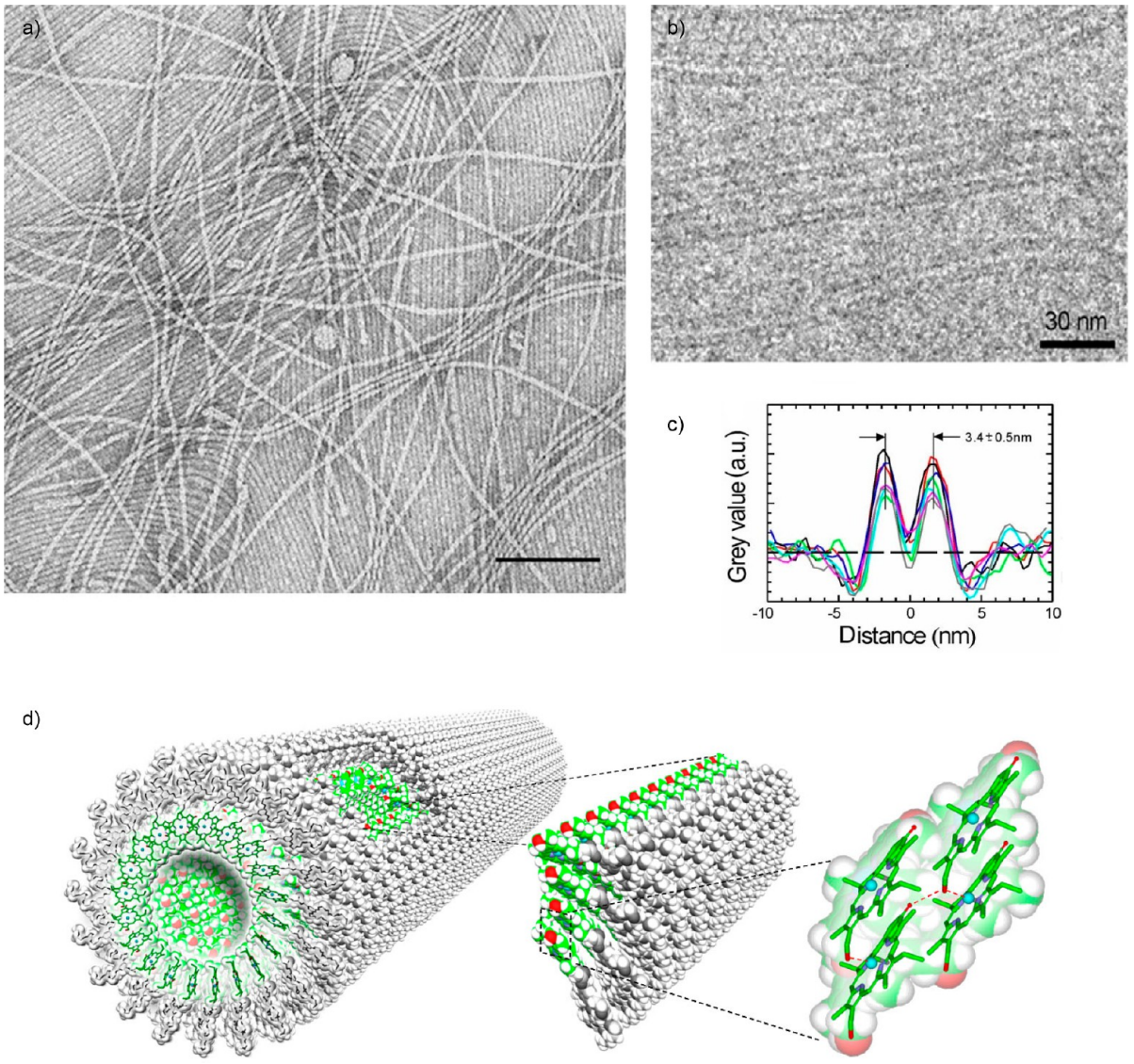

FIGURE 5. (a) TEM micrograph of **3** aggregates in water/methanol (100:1; v/v) with 0.5% uranyl acetate, scale bar 100 nm; (b) cryo-TEM micrograph of a 5×10^{-6} mol L^{-1} solution of **3** in water/methanol (100:1) showing tubular aggregates embedded in vitrified ice; (c) overlaid line scans across seven individual tubes; (d) schematic model of self-assembled nanotubes of **3**. Adapted from ref 35 with permission.

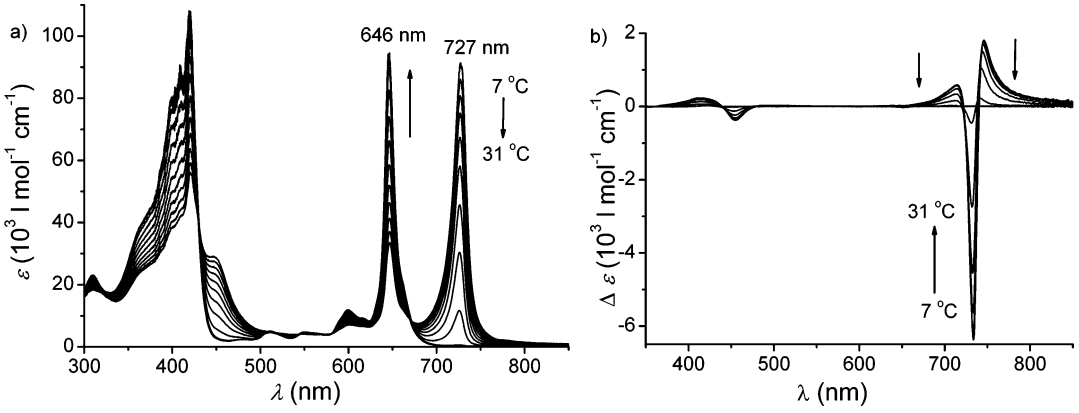

FIGURE 6. Temperature-dependent (a) UV/vis and (b) CD spectra of **2** in cyclohexane/*n*-hexane (1:1). Adapted from ref 26 with permission.

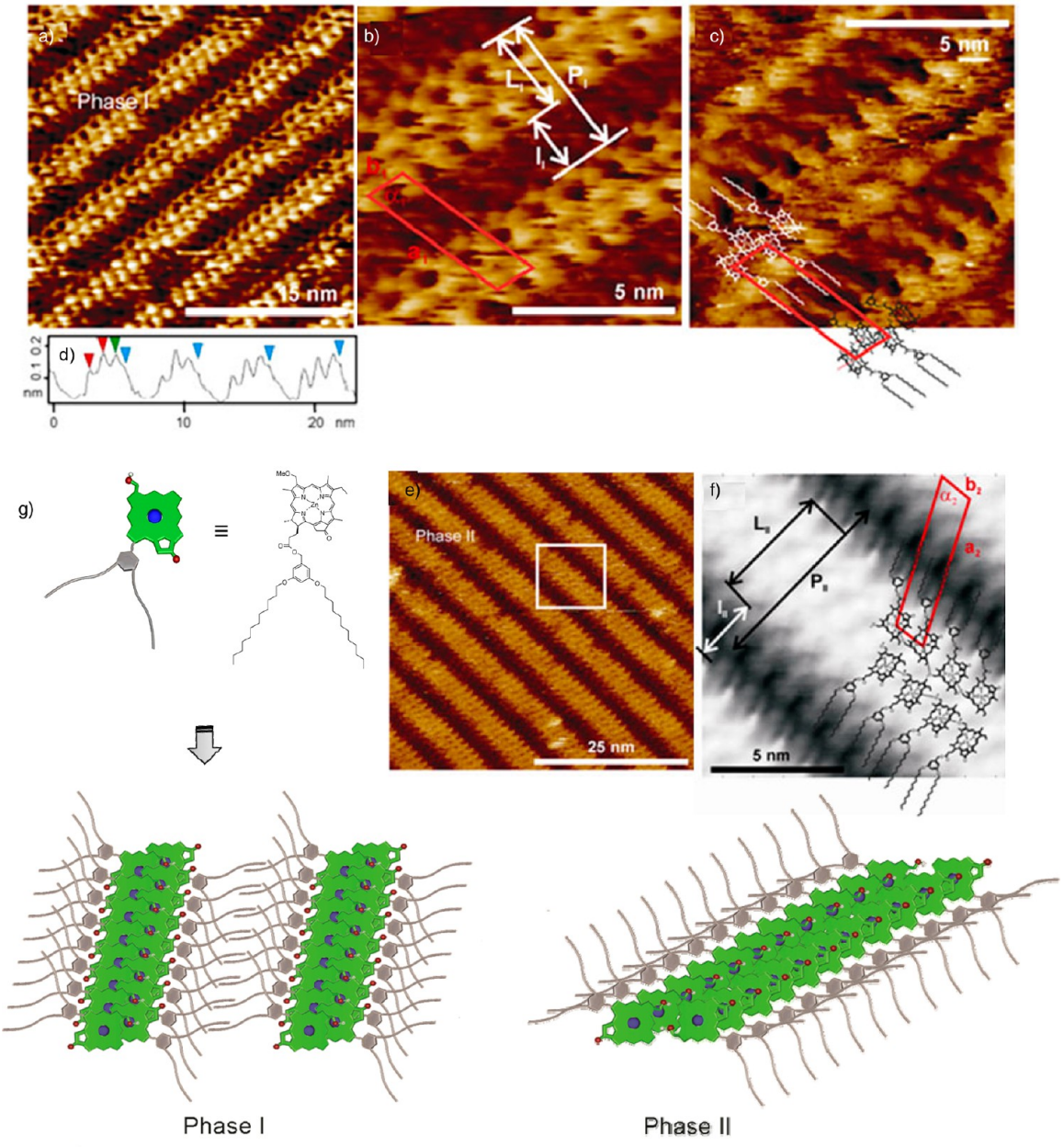

FIGURE 7. STM image of phase I arrangement of **2**: (a) V_{bias} −900 mV, *I* 5 pA; (b) magnified area of panel a; (c) V_{bias} −1100 mV, *I* 500 fA, with antiparallel arrangement of **2** in phase I; (d) cross section of four rows in panel a; (e) STM image of phase II arrangement of **2** (V_{bias} −2700 mV, *I* 500 fA); (f) parallel arrangement of **2** in phase II; (g) schematic representation of ZnChl **2** and π-stacks of **2** in phases I and II. Adapted from ref 26 with permission.

nanorods with excellent solubility in nonpolar solvents, whereas amphiphilic **3** functionalized with hydrophilic OEG chains form similar nanorods in aqueous media.[23,24] The spectral features of these aggregates, namely, a red-shifted Q_y-band from 647 nm (monomers) to 741 nm (aggregates) for **1** closely match those of BChl *c*−*e* aggregates in natural chlorosomes.[7] Temperature-variable UV/vis spectroscopy of ZnChl **1** and **4a**,**b** revealed thermodynamically reversible self-assembly of monomers into extended aggregates (Figure 3a). The CD spectra of these dye aggregates show bisignate signals in the region of aggregate Q_y-band as a result of an induced CD effect through excitonic coupling of the transition dipole moments of inherently chiral ZnChls (Figure 3b).[23−25] The formation of one-dimensional extended aggregates and wide polydispersity in aggregate size distribution in solution was evident by angle-dependent dynamic light scattering (DLS) studies (Figure 3c). For ZnChl **4b**, the dye aggregates could be stabilized by

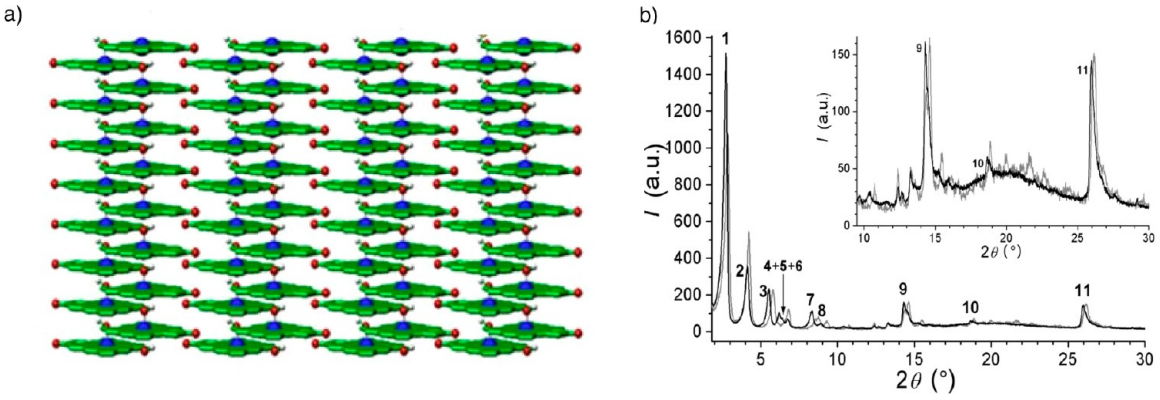

FIGURE 8. (a) Schematic representation of antiparallel packing model; (b) XRD pattern of **2** at room temperature (gray lines) and 80 °C (black lines). Inset shows an enlarged plot of wide angle region showing the crystalline order. Adapted from ref 37 with permission.

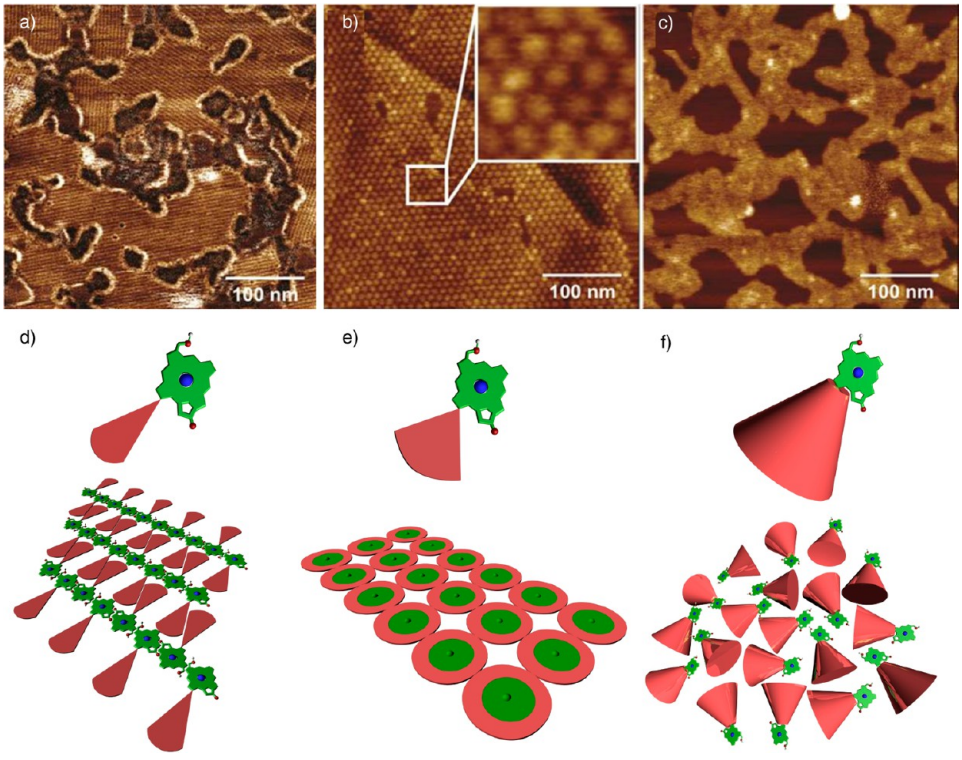

FIGURE 9. (a–c) AFM images of **5**, **6**, and **7** on HOPG, respectively: (a) phase image of **5**; (b, c) height images of **6** and **7**. Inset in panel b magnification of the area in the white box; (d–f) schematic illustrations of molecules **5**–**7** with particular shape and resulting self-assembled adlayers on HOPG. Adapted from ref 30 with permission.

olefin metathesis reaction, providing more stiff nanorods that did not disassemble upon addition of polar solvents or at elevated temperature.[25]

The morphological features of ZnChl **1** and **3** assemblies were studied by AFM on highly oriented pyrolytic graphite (HOPG) (Figure 4a–d) and on mica (Figure 4e,f) surfaces, which revealed well-defined nanoscale rod aggregates with uniform heights of ~5–6 nm.

Recently, we obtained unequivocal experimental evidence for the hollow tubular nature of these nanorod assemblies by transmission electron microscopy (TEM) (Figure 5a). Furthermore, a near-native solvated state of aggregates of **3** was preserved by cryogenic vitrification. Subsequent imaging by low-dose cryo-TEM enabled visualization of well-defined nanotubes of **3** in solution with wall maxima at a distance of 3.4 nm, total tube diameter of ~6 nm, and a central channel of ~2 nm (Figure 5b,c).[35]

The diameters (~5–6 nm) of these nanotubular assemblies are in excellent agreement with the EM data of chlorosomal BChl *c* rods (*Chloroflexus aurantiacus*)[36] and with

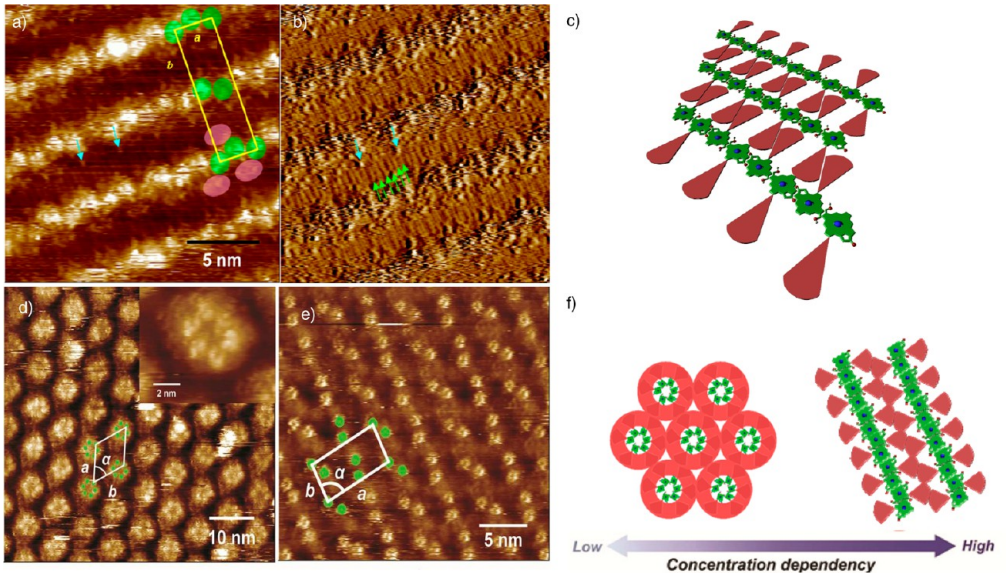

FIGURE 10. (a) STM height image of **5** at phenyloctane–HOPG interface, $V_{bias} = -1500$ mV, $I = 6$ pA; (b) current image of panel a, $V_{bias} = -900$ mV, $I = 5$ pA; (c) schematic model showing antiparallel rows of **5**; (d, e) STM images of **6** at different concentrations in 1-phenyloctane/octanoic acid (1:1); (f) schematic illustrations of the corresponding molecular arrangements in panels d and e. Adapted from ref 30 with permission.

the tubular model proposed by Holzwarth and Schaffner (Figure 5d).[17] Albeit for an artificial system, these results constitute the first unambiguous proof for the tubular arrangement of BChl derivatives.

4. Stack Assemblies: Solution, Surface, and Solid-State Characterization

Self-assembly of ZnChls could be tuned by substitution of the 3^1-hydroxy group with a methoxy group as in **2**, thereby obviating the possibility of interstack hydrogen bonding. Indeed, ZnChl **2** self-assembles into one-dimensional (1D) π-stacks in nonpolar solvents instead of nanotubules by virtue of $\pi-\pi$ stacking and coordination of 3^1-methoxy group to the central zinc ion.[26] The reversible formation of extended π-stacks was confirmed by temperature-dependent UV/vis measurements in cyclohexane/hexane (1:1) where a pronounced bathochromic shift of the Q_y-band from 646 nm (monomers) to 727 nm (aggregates) characteristic for J-type excitonic coupling (Figure 6a) was observed. A pronounced CD effect with two positive and one negative maxima (Figure 6b) indicates excitonic coupling of transition dipole moments of intrinsically chiral ZnChls.

AFM and scanning tunneling microscopy (STM) studies confirmed that **2** self-assembles into well-ordered π-stacks on the HOPG surface. Depending on sample concentrations either single or double stack aggregates are formed with rarely observed "edge-on" packing mode of ZnChls (Figure 7). At lower concentrations of **2** ($c = 10^{-7}$ M, phase I), alternating broad lamellae ($L_I = 2.8 \pm 0.1$ nm) and small lamellae ($l_I = 1.9 \pm 0.1$ nm) were observed with a periodicity (P_I) of 4.7 nm (Figure 7a–d), whereas at higher concentrations ($c = 10^{-5}$ M, phase II), extended broad lamellae ($L_{II} = 3.6 \pm 0.2$ nm) and small lamellae (l_{II}) similar to l_I were observed with a periodicity (P_{II}) of 5.6 nm (Figure 7e,f). Based on these observed dimensions, schematic models for the organization of **2** in phases I and II are depicted in Figure 7g, where phase I consists of single stacks of antiparallel-oriented **2**, while phase II consists of double stacks of parallel-oriented **2** molecules with alkyl chains of one stack arranged in the same direction.

Recently, the molecular packing of self-assembled ZnChls **1** and **2** in the solid state has been elucidated by magic angle spinning (MAS) NMR in conjunction with powder X-ray diffraction (XRD), DFT calculations, and molecular modeling studies.[37] The experimental NMR shifts of aggregates of **1** and **2** were reproduced by DFT-based ring-current shift calculations for the antiparallel stacking model (Figure 8a). Small-angle XRD (Figure 8b) confirmed the crystallinity of the assembly of **2**, and the local antiparallel model derived from solid-state NMR was extended to a three-dimensional (3D) periodic packing in line with XRD results, providing a conclusive brickwork-type short-range structural arrangement of **2** in the solid state.[37] Theoretical studies suggested that the inherent chirality and precise stereochemical orientation of ZnChl **2** in the stack strongly influences the observed CD spectra (Figure 6b).[38]

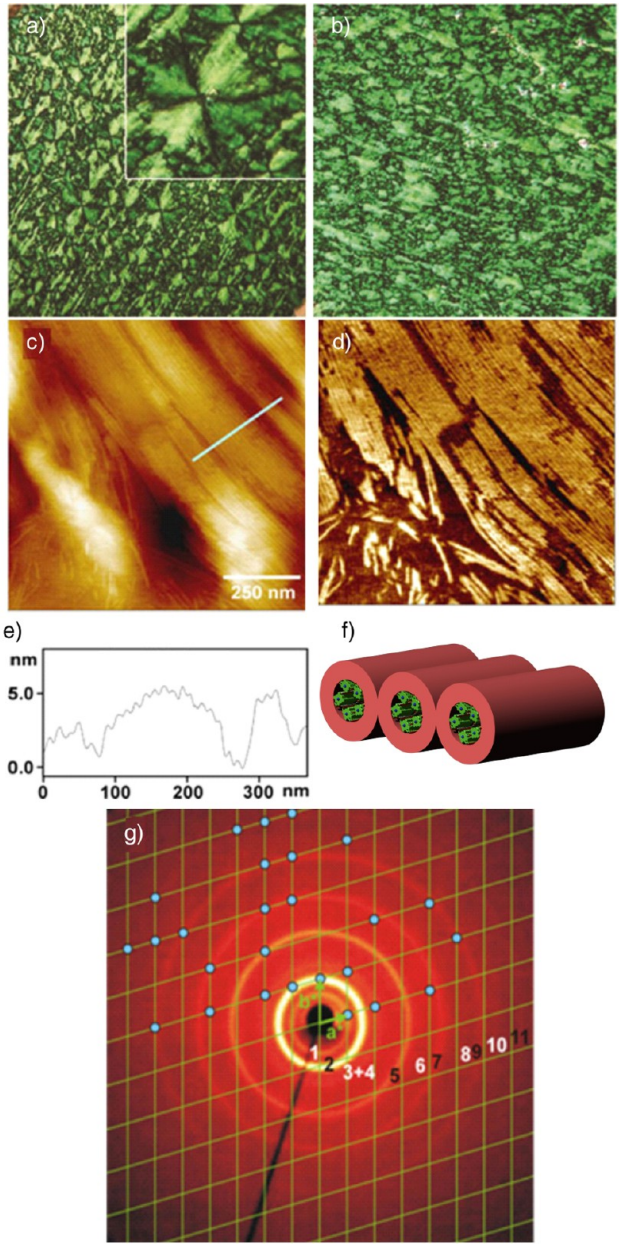

FIGURE 11. (a, b) Spherulitic textures of **6** under crossed polarizers of POM before and after shearing; (c) AFM height image of **6** on glass upon cooling from isotropic melt; (d) corresponding phase image; (e) cross section of the blue line in panel c; (f) pictorial representation of columns with width of ~10 nm; (g) indexing of small-angle XRD reflections of **6** to a 2D oblique lattice with $a = 83.5$ Å, $b = 56.9$ Å, and $\gamma = 106.0°$. Adapted from ref 31 with permission.

5. Dendron-Mediated Self-Assembly: Surface Packing and Liquid Crystalline (LC) Phases

Based on the second design strategy discussed in section 2, self-assembly of ZnChls was tuned by subtle change of substituents in the ester group at 17[2]-position such as attachment of second generation "Percec-type" dendrons.[30,31] The steric restrictions and shapes of the second generation (G2) dendron wedges attached to ZnChls **5**–**7** (Scheme 1) have pronounced influence on surface organization of these dyes but inhibited their self-assembly in solution. AFM studies showed that **5** with the smallest wedge in the series self-assembles into a lamellar arrangement (Figure 9a,d) onto HOPG, whereas compound **7** with the largest wedge in the series is completely inhibited for organization on HOPG (Figure 9c,f) or in the solid state.[31] Interestingly, only the size of the dendron **6** is effective for the formation of ordered cyclic nanostructures (Figure 9b,e).

STM studies of **5** at phenyloctane–HOPG interface revealed antiparallel molecular arrangement within the lamellae, the brighter spots being attributed to chlorin cores, the feeble bright areas to phenyl rings of the dendrons (Figure 10a), and the striations in the dark trough to dodecyl chains of the dendrons (Figure 10b). Accordingly, a tentative model for the "face-on" molecular ordering of **5** with unit cell parameters $a = 2.65 \pm 0.10$ nm, $b = 9.40 \pm 0.19$ nm, and $\alpha = 92° \pm 2°$ was proposed (Figure 10c).

On the other hand, STM of **6** at the interface of 1-phenyloctane/octanoic acid (1:1) and HOPG showed highly ordered cyclic structures (Figure 10d) with each cycle consisting of six molecules corresponding to six bright spots (Figure 10d, inset) and a hexagonal unit cell with parameters $a = b = 7.37 \pm 0.08$ nm and $\alpha = 60° \pm 5°$. The cyclic adlayers are established solely by the 2D spatial demands of dendron.[30] At higher concentrations of **6** in 1-phenyloctane/octanoic acid (1:1), densely packed linear structures were observed at the solution–HOPG interface (Figure 10e). This behavior validates that the delicate balance of interactions between solvent, molecule, and substrate is highly important for 2D self-assembly of **6**.

For ZnChl **6**, spherulitic birefringent textures typical for columnar LC phases were observed under the crossed polarizers of POM (Figure 11a,b).[31] By AFM images of bulk samples, one-dimensional columns with diameters of ~10 nm were visualized (Figure 11c–e). Wide-angle XRD patterns of **6** exhibit medium to long-range order in the LC phases with typical π–π stacking of 3.5 Å, while the small-angle XRD reflections were indexed to a 2D oblique lattice (Figure 11g). The unit cell area calculated from lattice parameters of XRD ($A_{cell} = a \times b \times \sin \gamma = 4567.1$ Å^2) corroborated that from STM ($A_{cell} = a \times b \times \sin \gamma = 4704.0$ Å^2), although the calculated number of molecules in column cross section from X-ray ($n_{in} = 5$) appeared to be slightly smaller.[31] Based on these correlations, **6** was proposed to self-assemble into nanosegregated columns consisting of pentameric rosettes of π–π stacked ZnChls, and these columns further self-organize into a 2D oblique lattice.

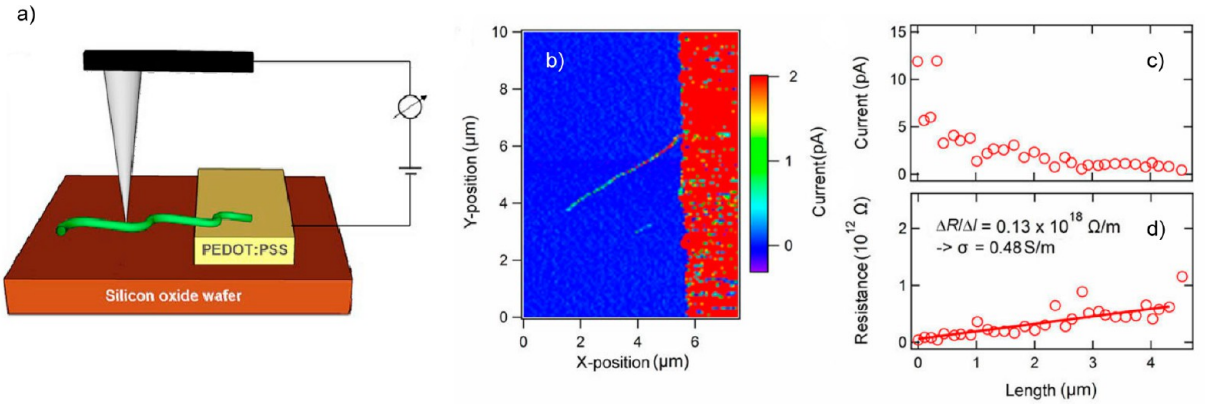

FIGURE 12. (a) Schematic illustration of conductive-AFM setup. (b) Current image ($7.5 \times 10\,\mu m^2$) of **3** nanowire adsorbed onto silicon oxide; the wire is connected to a thin layer of conductive polymer (PEDOT/PSS) in the right part of image. (c) Current vs length and (d) resistance vs length plots of nanowires of **3**. Nanowire conductivity is determined from the slope of resistance vs length plot. Adapted from ref 35 with permission.

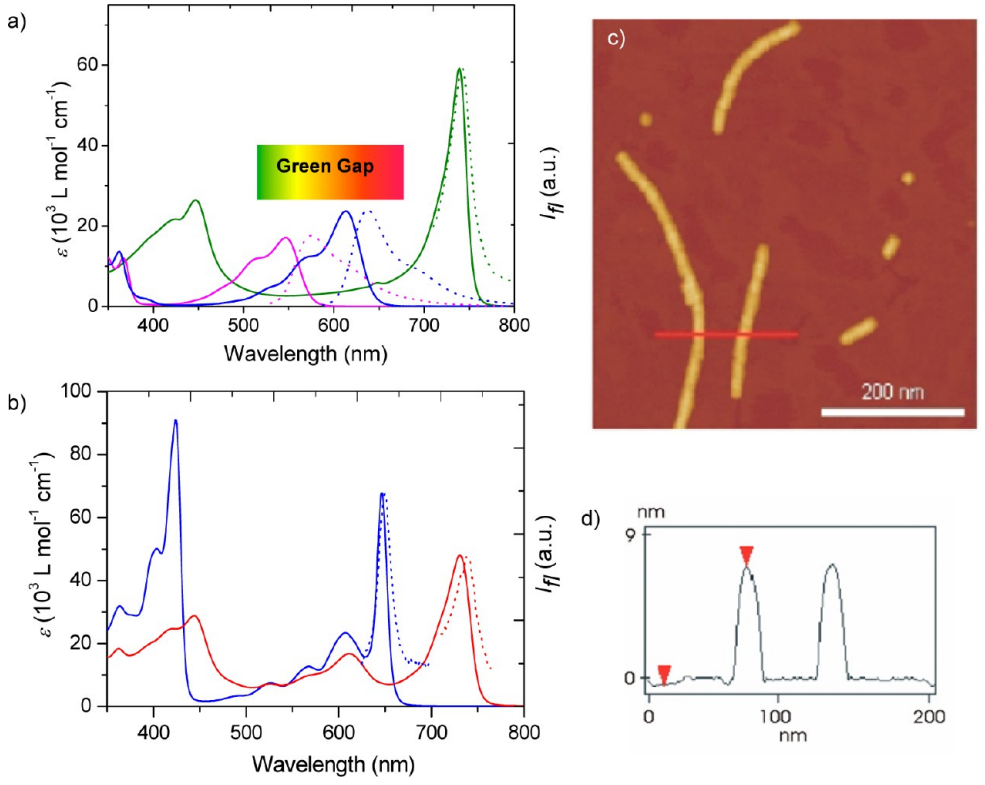

FIGURE 13. (a) UV/vis spectra (solid lines) and normalized fluorescence spectra (dotted lines) in cyclohexane/tetrachloromethane (100:1; v/v) of ZnChl **1** aggregates (green lines) indicating spectral "green gap", pink NBI (pink lines), and blue NBI (blue lines). (b) UV/vis (solid lines) and normalized fluorescence (dashed lines) of ZnChl–NBI **8** monomers in THF (blue lines) and aggregates in cyclohexane/tetrachloromethane (100:1) (red lines). (c) AFM image of **8** prepared by spin-coating of a cyclohexane/THF (100:1; v/v) solution onto HOPG and (d) height profile along the red line in panel c. Adapted from refs 32 and 33 with permission.

6. Charge Transport in Tubular, Stack, and LC Assemblies of ZnChls: Toward Biosupramolecular Electronics

The inherent ability of unidimensional nanostructures, such as nanorods and tubes,[39] and columnar discotic liquid crystals (DLCs) to serve as charge transport conduits is well-established.[40,41] Owing to their highly organized structures in solution and in solid state, assemblies of ZnChls **1**–**6** are envisioned to serve as conductive nanosized 1D wires. Toward this goal, intrinsic charge transport properties of **1**–**4** and **6** in the solid state were studied using the electrodeless pulse radiolysis time-resolved microwave

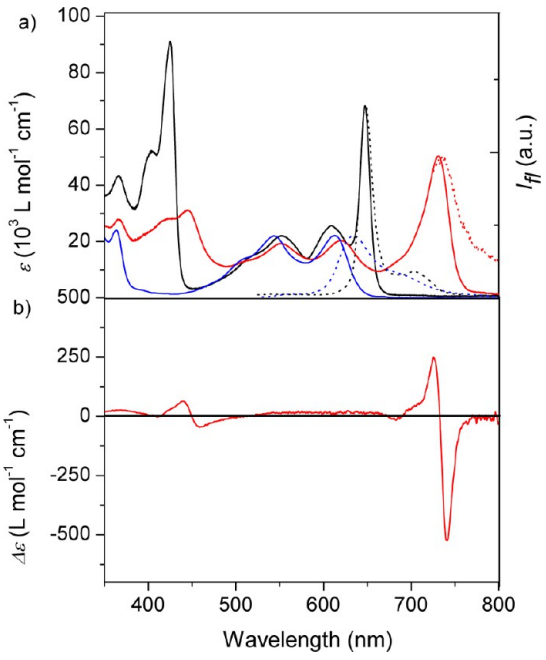

FIGURE 14. (a) UV/vis (solid lines) and normalized fluorescence spectra (dotted lines) of triad **10** monomers in THF (black) and its aggregates in cyclohexane/tetrachloromethane (100:1; v/v) (red) and respective NBI-NBI dyad reference (blue) in cyclohexane/tetrachloromethane (100:1; v/v); (b) CD spectrum of aggregates of **10**. Adapted from ref 33 with permission.

conductivity (PR-TRMC) technique.[41] Appreciable charge carrier mobilities of ~0.03−0.07 $cm^2/(V\,s)$ at room temperature (RT) were found in tubular assemblies of **1**, **3**, and **4a** and up to 0.1 $cm^2/(V\,s)$ at elevated temperatures, indicating thermally activated charge transport in tubular assemblies. On the other hand, stack assemblies of **2** exhibited even higher mobilities of up to 0.28 $cm^2/(V\,s)$ at RT.[42] If we consider that the slipped-stack arrangement of these chlorin derivatives offers only partial overlap of the neighboring π-scaffolds, these values are indeed quite impressive. They are several orders of magnitude larger than those reported to date for less organized chlorophylls[13] or well-ordered liquid crystalline porphyrins[43] and even approach the record values observed for highly organized columnar stacks of hexabenzocoronenes (0.4 $cm^2/(V\,s)$ for the liquid-crystalline phase and 1 $cm^2/(V\,s)$ for the crystalline phase at RT),[44] which are larger π-scaffolds and whose cofacial arrangement offers by far larger π-contact surfaces between neighboring molecules.

Distinct differences in charge transport properties of tubular and stack assemblies[42] correspond well with their macroscopic organization derived from spectroscopic, crystallographic, and microscopic studies. For liquid crystalline ZnChl **6**, comparatively low charge carrier mobilities of ~10^{-3}−10^{-2} $cm^2/(V\,s)$ were obtained in the mesophase temperature range where a less ordered stacking of the dyes without metallosupramolecular ligation prevails.[31] First-order decay and long lifetimes of PR-TRMC transients suggest charge recombination via intercolumnar tunneling through insulating hydrocarbon mantles,[31] similar to that observed for DLCs.[41,44]

Although one-dimensional self-assemblies in the length scale of 10−100 nm are suitable for nanoelectronic component design, it is challenging to develop methodologies to establish their contacts to electrodes in order to construct nanocircuits. Recently, electrical conductivity of tubular assemblies of **3** has been proven[35] by employing a conductive-AFM (*current*-AFM, Figure 12a) technique. Owing to their hydrophilicity, tubular assemblies of **3** could be aligned onto nonconductive mica or silicon oxide substrates. Subsequently, they were contacted by a conductive polymer PEDOT/PSS. The topography was then measured in contact mode AFM with a conductive tip. A bias voltage was applied between the conductive polymer and the conductive tip during scanning and the resulting current that flows between tip and sample was measured with an external current amplifier. The signals in current image (Figure 12b) reveal that ZnChl nanowires are indeed electrically conductive. The measured current and resistance were analyzed as a function of length of the nanowires, and the latter showed a linear relationship with length, which allowed a quantitative determination of their conductivity using Ohm's law (Figure 12c,d). Based on electron microscopic results, tubular wires of **3** with radii *r* of ~3 nm were considered, and these nanowires were found to exhibit high conductivity of 0.48 S/m.

7. Multichromophoric ZnChl−NBI Conjugates for Energy Transfer

It is remarkable that most natural LH systems lack the dyes required for efficient absorption of solar radiation between 500 and 600 nm (so-called "green gap"). To efficiently harvest the green light of the solar spectrum, multichromophoric zinc chlorins were synthesized by employing the third design strategy. Biomimetic LH systems based on ZnChl−NBI conjugates **8**−**10** that contain blue and pink colored NBIs were achieved. The latter act as LH chromophores in the green region (Figure 13a), thereby covering the spectral "green gap".[32,33] The self-assembly properties of ZnChl−NBI dyads **8** and **9** and triad **10** have been studied in nonpolar aprotic solvents cyclohexane/tetrachlomethane (100:1) by UV/vis, CD, and steady-state emission spectroscopy (Figures 13b and 14), revealing extended aggregates of ZnChl−NBI dyads and triad. AFM investigations validated

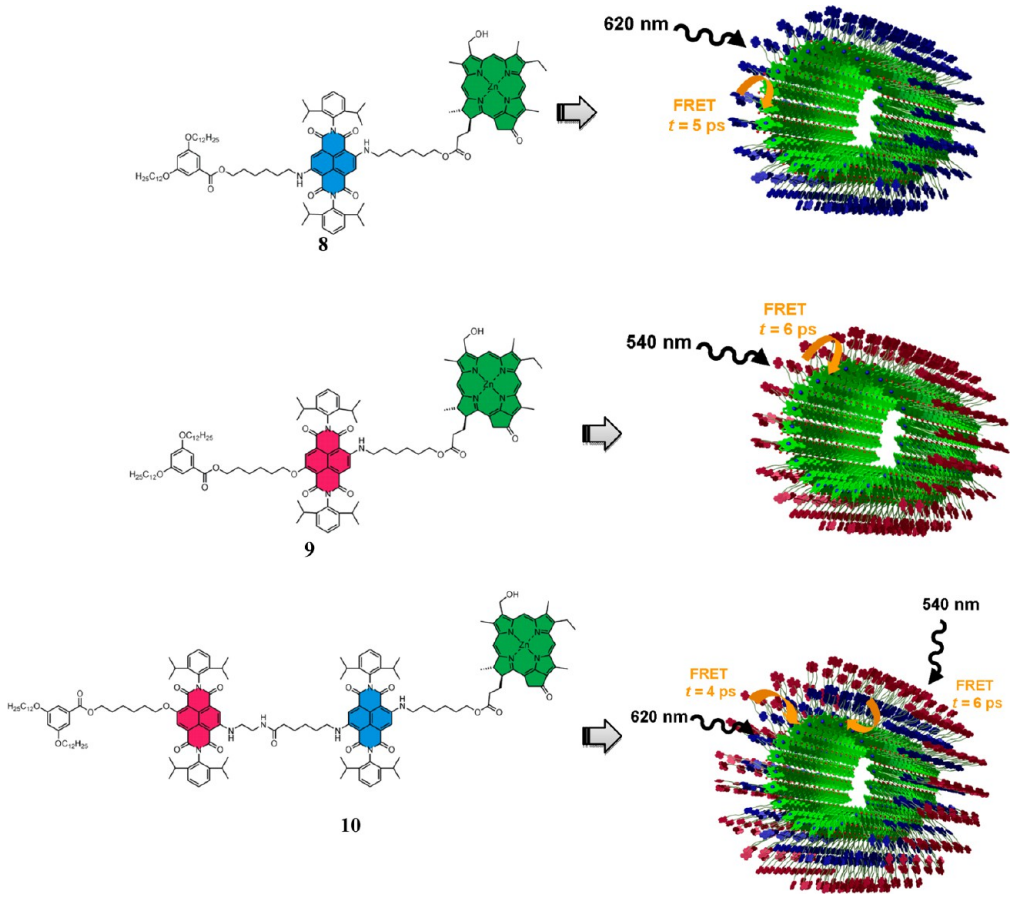

FIGURE 15. Schematic illustration of self-assembly of ZnChl–NBI dyads **8** and **9** and triad **10** into rod-like assemblies and the FRET processes upon selective photoexcitation of different NBIs. Adapted from ref 33 with permission.

the formation of extended rod assemblies of ~7.3 nm height that are formed by noncovalent interactions of ZnChls, while the appended NBIs at the periphery do not aggregate (Figure 13c, d).[32,33]

The photophysical and energy transport properties of monomers and aggregates of **8**–**10** were investigated by time-resolved fluorescence experiments. In all the monomers, photoexcitation of NBIs leads to highly efficient fluorescence resonance energy transfer (FRET) processes to the ZnChl on the picosecond time scale (7–25 ps). Upon selective photoexcitation of the enveloping blue and pink NBI units of aggregates of **8**–**10** at 620 and 540 nm, respectively, their excitation energy is quantitatively conveyed to ZnChl backbone with even faster energy transfer time constants (5–6 ps). The efficiencies of ZnChl rod aggregates for harvesting of solar light are markedly increased from 26% for dyad **8** up to 63% for triad **10**, compared with the LH capacity of the monochromophoric aggregates of ZnChl **1**. The self-assembly of dyads **8** and **9** and triad **10** into nanorods and rapid energy transport processes (~4–6 ps) from peripheral NBIs into ZnChls upon selective photoexcitation of peripheral pink and blue NBIs are schematically represented in Figure 15. These systems are highly sophisticated self-organized multichromophoric light-harvesting antennae mimicking natural LH systems.

8. Summary and Perspective

To summarize, ZnChls functionalized at the 3^1-position with a hydroxy or methoxy group have been tailored for different modes of self-assembly into tubes, stacks, and lamellae with well-defined structures and desirable optical and electronic properties. Beyond the functional properties of their natural counterparts, we could demonstrate that the slipped π-stack arrangement imparted by the ligation of the hydroxyl functional group to the zinc ion in the center of the chlorin scaffold provides also an excellent contact for charge carrier transport that indeed rivals the best organic semiconductor molecules. Self-assembly of such ZnChls could be tuned by peripheral dendron functionalization that afforded well-defined linear and cyclic surface adlayers

and novel LC materials with appreciable charge transport properties. ZnChls covalently linked with NBIs act as LH chromophores covering the spectral "green gap" whose LH efficiency for the absorption of terrestrial sunlight was increased by up to 63% compared with the monochromophoric ZnChl rod assemblies. These studies have unraveled important structural and functional features of biomimetic ZnChl assemblies justifying their prospects as artificial chlorosomes and contribute to the knowledge base that is a prerequisite for bottom-up fabrication of nanoelectronic devices. Thus, molecular design and self-assembly principles can be combined to achieve materials driven from natural sources, here chlorophylls, with (opto-)electronic properties desirable for supramolecular electronic and photonic device fabrication. We anticipate that the results discussed in this Account on nanostructures based on chlorophyll scaffolds will promote the area of biosupramolecular electronics.

Financial support by the Volkswagen Foundation and the Bavarian State Ministry of Science, Research, and the Arts is gratefully acknowledged. The work described is the collective efforts of the past and present co-workers of F.W., whose names appear in different cited references, and we express our sincere gratitude to them. Collaborating groups are greatly acknowledged.

BIOGRAPHICAL INFORMATION

Sanchita Sengupta studied chemistry at the Indian Institute of Technology (IIT), Kanpur, where she received her Master degree in 2006. Subsequently, she joined the group of Frank Würthner at Universität Würzburg where she obtained the doctoral degree in 2011 for her studies on the self-assembly of zinc chlorins. After a postdoctoral stay at the Department of Chemical Engineering, Delft University of Technology, Netherlands, she became an assistant professor at the Indian Institute of Science in Bangalore, India, in 2013.

Frank Würthner studied chemistry at Universität Stuttgart, Germany, where he received the doctoral degree in 1993. After postdoctoral research at MIT in Cambridge (USA), two years at BASF Central Research in Ludwigshafen, and a Habilitation in Organic Chemistry at Universität Ulm (2001), he became full professor at Universität Würzburg in 2002. His research interests include dye chemistry, noncovalent synthesis of functional nanostructures, and applications of organic materials in electronics and photonics.

FOOTNOTES

*To whom correspondence should be addressed. E-mail: wuerthner@chemie.uni-wuerzburg.de.
The authors declare no competing financial interest.
§S.S.: Indian Institute of Science, Bangalore 560012, India.

REFERENCES

1 McDermott, G.; Prince, S. M.; Freer, A. A.; Hawthornthwaite-Lawless, A. M.; Papiz, M. Z.; Cogdell, R. J.; Isaacs, N. W. Crystal-structure of an integral membrane light-harvesting complex from photosynthetic bacteria. *Nature* **1995**, *374*, 517–521.

2 Cogdell, R. J.; Gall, A.; Köhler, J. The architecture and function of the light-harvesting apparatus of purple bacteria: From single molecules to in vivo membranes. *Q. Rev. Biophys.* **2006**, *39*, 227–324.

3 Wasielewski, M. R. Self-assembly strategies for integrating light harvesting and charge separation in artificial photosynthetic systems. *Acc. Chem. Res.* **2009**, *42*, 1910–1921.

4 Balaban, T. S. Tailoring porphyrins and chlorins for self-assembly in biomimetic artificial antenna systems. *Acc. Chem. Res.* **2005**, *38*, 612–623.

5 You, C.-C.; Dobrawa, R.; Saha-Möller, C. R.; Würthner, F. Metallosupramolecular dye assemblies. *Top. Curr. Chem.* **2005**, *258*, 39–82.

6 Aratani, N.; Kim, D.; Osuka, A. Discrete cyclic porphyrin arrays as artificial light-harvesting antenna. *Acc. Chem. Res.* **2009**, *42*, 1922–1934.

7 Balaban, T. S.; Tamiaki, H.; Holzwarth, A. R. Chlorins programmed for self-assembly. *Top. Curr. Chem.* **2005**, *258*, 1–38.

8 Tamiaki, H. Self-aggregates of natural and modified chlorophylls as photosynthetic light-harvesting antenna systems: substituent effect on the B-ring. *Photochem. Photobiol. Sci.* **2005**, *4*, 675–680.

9 Bryant, D. A.; Costas, A. M. G.; Maresca, J. A.; Chew, A. G. M.; Klatt, C. G.; Bateson, M. M.; Tallon, L. J.; Hostetler, J.; Nelson, W. C.; Heidelberg, J. F.; Ward, D. M. *Candidatus Chloracidobacterium thermophilum*: An aerobic phototrophic acidobacterium. *Science* **2007**, *317*, 523–526.

10 Saga, Y.; Shibata, Y.; Itoh, S.; Tamiaki, H. Direct counting of submicrometer-sized photosynthetic apparatus dispersed in medium at cryogenic temperature by confocal laser fluorescence microscopy. *J. Phys. Chem. B* **2007**, *111*, 12605–12609.

11 Würthner, F.; Kaiser, T. E.; Saha-Möller, C. R. J-Aggregates: From serendipitous discovery to supramolecular engineering of functional dye materials. *Angew. Chem., Int. Ed.* **2011**, *50*, 3376–3410.

12 Scholes, G. D.; Rumbles, G. Excitons in nanoscale systems. *Nat. Mater.* **2006**, *5*, 683–696.

13 Kassi, H.; Leblanc, R. M.; Hotchandani, S. Hole mobility in microcrystalline chlorophyll a. *Phys. Status Solidi B* **2000**, *220*, 931–939.

14 Hu, X.; Schulten, K. How nature harvests sunlight. *Phys. Today* **1997**, *50*, 28–34.

15 Bahatyrova, S.; Frese, R. N.; Siebert, C. A.; Olsen, J. D.; van der Werf, K. O.; van Grondelle, R.; Niederman, R. A.; Bullough, P. A.; Otto, C.; Hunter, C. N. The native architecture of a photosynthetic membrane. *Nature* **2004**, *430*, 1058–1062.

16 Oostergetel, G. T.; van Amerongen, H.; Boekema, E. J. The chlorosome: A prototype for efficient light harvesting in photosynthesis. *Photosynth. Res.* **2010**, *104*, 245–255.

17 Holzwarth, A. R.; Schaffner, K. On the structure of bacteriochlorophyll molecular aggregates in the chlorosomes of green bacteria. A molecular modeling study. *Photosyn. Res.* **1994**, *41*, 225–233.

18 Pšenčík, J.; Ikonen, T. P.; Laurinmäki, P.; Merckel, M. C.; Butcher, S. J.; Serimaa, R. E.; Tuma, R. Lamellar organization of pigments in chlorosomes, the light harvesting complexes of green photosynthetic bacteria. *Biophys. J.* **2004**, *87*, 1165–1172.

19 Oostergetel, G. T.; Reus, M.; Chew, A. G. M.; Bryant, D. A.; Boekema, E. J.; Holzwarth, A. R. Long-range organization of bacteriochlorophyll in chlorosomes of chlorobium tepidum investigated by cryo-electron microscopy. *FEBS Lett.* **2007**, *581*, 5435–5439.

20 Ganapathy, S.; Oostergetel, G. T.; Wawrzyniak, P. K.; Reus, M.; Chew, A. G. M.; Buda, F.; Boekema, E. J.; Bryant, D. A.; Holzwarth, A. R.; de Groot, H. J. M. Alternating syn-anti bacteriochlorophylls form concentric helical nanotubes in chlorosomes. *Proc. Natl. Acad. Sci. U. S. A.* **2009**, *106*, 8525–8530.

21 Ganapathy, S.; Oostergetel, G. T.; Reus, M.; Tsukatani, Y.; Chew, A. G. M.; Buda, F.; Bryant, D. A.; Holzwarth, A. R.; de Groot, H. J. M. Structural variability in wild-type and bchQ bchR mutant chlorosomes of the green sulfur bacterium chlorobaculum tepidum. *Biochemistry* **2012**, *51*, 4488–4498.

22 Tamiaki, H.; Amakawa, M.; Shimono, Y.; Tanikaga, R.; Holzwarth, A. R.; Schaffner, K. Synthetic zinc and magnesium chlorin aggregates as models for supramolecular antenna complexes in chlorosomes of green photosynthetic bacteria. *Photochem. Photobiol.* **1996**, *63*, 92–99.

23 Huber, V.; Katterle, M.; Lysetska, M.; Würthner, F. Reversible self-organization of semisynthetic zinc chlorins into well-defined rod antennae. *Angew. Chem., Int. Ed.* **2005**, *44*, 3147–3151.

24 Huber, V.; Sengupta, S.; Würthner, F. Structure-property relationships for self-assembled zinc chlorin light-harvesting dye aggregates. *Chem.—Eur. J.* **2008**, *14*, 7791–7807.

25 Sengupta, S.; Würthner, F. Covalently stabilized self-assembled chlorophyll nanorods by olefin metathesis. *Chem. Commun.* **2012**, *48*, 5730–5732.

26 Huber, V.; Lysetska, M.; Würthner, F. Self-assembled single- and double-stack π-aggregates of chlorophyll derivatives on highly ordered pyrolytic graphite. *Small* **2007**, *3*, 1007–1014.

27 Miyatake, T.; Tanigawa, S.; Katoa, S.; Tamiaki, H. Aqueous self-aggregates of amphiphilic zinc 3^1-hydroxy- and 3^1-methoxy-chlorins for supramolecular light-harvesting systems. *Tetrahedron Lett.* **2007**, *48*, 2251–2254.

28 Shoji, S.; Hashishin, T.; Tamiaki, H. Construction of chlorosomal rod self-aggregates in the solid state on any substrates from synthetic chlorophyll derivatives possessing an oligomethylene chain at the 17-propionate residue. *Chem.—Eur. J.* **2012**, *18*, 13331–13341.

29 Rosen, B. M.; Wilson, C. J.; Wilson, D. A.; Peterca, M.; Imam, M. R.; Percec, V. Dendron-mediated self-assembly, disassembly, and self-organization of complex systems. *Chem. Rev.* **2009**, *109*, 6275–6540.

30 Uemura, S.; Sengupta, S.; Würthner, F. Cyclic self-assembled structures of chlorophyll dyes on HOPG by dendron wedge effect. *Angew. Chem., Int. Ed.* **2009**, *48*, 7825–7828.

31 Sengupta, S.; Uemura, S.; Patwardhan, S.; Huber, V.; Grozema, F. C.; Siebbeles, L. D. A.; Baumeister, U.; Würthner, F. Columnar mesophases based on zinc chlorophyll derivatives functionalized with peripheral dendron wedges. *Chem.—Eur. J.* **2011**, *17*, 5300–5310.

32 Röger, C.; Müller, M. G.; Lysetska, M.; Miloslavina, Y.; Holzwarth, A. R.; Würthner, F. Efficient energy transfer from peripheral chromophores to the self-assembled zinc chlorin rod antenna: a bioinspired light-harvesting system to bridge the "green gap". *J. Am. Chem. Soc.* **2006**, *128*, 6542–6543.

33 Röger, C.; Miloslavina, Y.; Brunner, D.; Holzwarth, A. R.; Würthner, F. Self-assembled zinc chlorin rod antennae powered by peripheral light-harvesting chromophores. *J. Am. Chem. Soc.* **2008**, *130*, 5929–5939.

34 Smith, K. M.; Goff, D. A.; Simpson, D. J. Meso-substitution of chlorophyll derivatives: direct route for transformation of bacteriopheophorbides-d into bacteriopheophorbides-c *J. Am. Chem. Soc.* **1985**, *107*, 4946–4954.

35 Sengupta, S.; Ebeling, D.; Patwardhan, S.; Zhang, X.; von Berlepsch, H.; Böttcher, C.; Stepanenko, V.; Uemura, S.; Hentschel, C.; Fuchs, H.; Grozema, F. C.; Siebbeles, L. D. A.; Holzwarth, A. R.; Chi, L.; Würthner, F. Biosupramolecular nanowires from chlorophyll dyes with exceptional charge-transport properties. *Angew. Chem., Int. Ed.* **2012**, *51*, 6378–6382.

36 Sprague, S. G.; Staehelin, L. A.; DiBartolomeis, M. J.; Fuller, R. C. Isolation and development of chlorosomes in the green bacterium chloroflexus-aurantiacus. *J. Bacteriol.* **1981**, *147*, 1021–1031.

37 Ganapathy, S.; Sengupta, S.; Wawrzyniak, P. K.; Huber, V.; Buda, F.; Baumeister, U.; Würthner, F.; de Groot, H. J. M. Zinc chlorins for artificial light-harvesting self-assemble into antiparallel stacks forming a microcrystalline solid-state material. *Proc. Natl. Acad. Sci. U. S. A.* **2009**, *106*, 11472–11477.

38 Patwardhan, S.; Sengupta, S.; Würthner, F.; Siebbeles, L. D. A.; Grozema, F. C. Theoretical study of the optical properties of artificial self-organizing zinc chlorins. *J. Phys. Chem. C* **2010**, *114*, 20834–20842.

39 Schenning, A. P. H. J.; Meijer, E. W. Supramolecular electronics; nanowires from self-assembled π-conjugated systems. *Chem. Commun.* **2005**, 3245–3258.

40 Grozema, F. C.; Siebbeles, L. D. A. Mechanism of charge transport in self organizing organic materials. *Int. Rev. Phys. Chem.* **2008**, *27*, 87–138.

41 Warman, J. M.; Van de Craats, A. M. Charge mobility in discotic materials studied by PR-TRMC. *Mol. Cryst. Liq. Cryst.* **2003**, *396*, 41–72.

42 Patwardhan, S.; Sengupta, S.; Siebbeles, L. D. A.; Würthner, F.; Grozema, F. C. Efficient charge transport in semisynthetic zinc chlorin dye assemblies. *J. Am. Chem. Soc.* **2012**, *134*, 16147–16150.

43 Schouten, P. G.; Warman, J. M.; de Haas, M. P.; Fox, M. A.; Pan, H.-L. Charge migration in supramolecular stacks of peripherally substituted porphyrins. *Nature* **1991**, *353*, 736–737.

44 van de Craats, A. M.; Warman, J. M.; Fechtenkötter, A.; Brand, J. D.; Harbison, M. A.; Müllen, K. Record charge carrier mobility in a room-temperature discotic liquid-crystalline derivative of hexabenzocoronene. *Adv. Mater.* **1999**, *11*, 1469–1472.